Spontaneous adaptation of ion selectivity in a bacterial flagellar motor

Pietro Ridone[1], Tsubasa Ishida[2], Yoshiyuki Sowa[2,3], Matthew A. B. Baker[1,4*]

[1]School of Biotechnology and Biomolecular Sciences, University of New South Wales, Sydney, Australia.

[2]Department of Frontier Bioscience, Hosei University, Tokyo, Japan.

[3]Research Center for Micro-Nano Technology, Hosei University, Tokyo, Japan.

[4]CSIRO Synthetic Biology Future Science Platform, Brisbane, Australia.

*correspondence: matthew.baker@unsw.edu.au

ABSTRACT

Motility provides a selective advantage to many bacterial species and is often achieved by rotation of flagella that propel the cell towards more favourable conditions. In most species, the rotation of the flagellum, driven by the Bacterial Flagellar Motor (BFM), is powered by H^+ or Na^+ ion transit through the torque-generating stator subunits of the motor complex. The ionic requirements for motility appear to have adapted to environmental changes throughout history but the molecular basis of this adaptation, and the constraints which govern the evolution of the stator proteins are unknown. Here we use CRISPR-mediated genome engineering to replace the native H^+-powered stator genes of *Escherichia coli* with a compatible sodium-powered stator set from *Vibrio alginolyticus* and subsequently direct the evolution of the stators to revert to H^+-powered motility. Evidence from whole genome sequencing indicates both flagellar- and non-flagellar-associated genes that are involved in longer-term adaptation to new power sources. Overall, transplanted Na^+- powered stator genes can spontaneously incorporate novel mutations that allow H^+-motility when environmental Na^+ is lacking.

INTRODUCTION

Bacterial motility via the flagellar motor represents one of the earliest forms of locomotion. This rotary motility imparts such significant selective advantage[1,2] that resources are allocated to chemotaxis even in the absence of nutrient gradients[3,4]. Furthermore, the evolutionary origins, and subsequent adaptation of the motor are of significant scientific and public interest[5], since the BFM holds prominence as an ancient, large, molecular complex of high sophistication.

The torque that drives the BFM is supplied by motor-associated transmembrane protein-complexes known as stators. The stator complex, an asymmetric heteroheptamer (in *E. coli:* $MotA_5MotA_2$) most likely acts itself as a miniature rotating nanomachine coupling ion transit to rotation[6,7]. The stators are essential for motility, as they drive rotation, and are accessible for studies in experimental evolution due to their unambiguous role in connecting a specific environmental cue (presence of the coupling ion) to an easily discernible phenotype (cell swimming). Furthermore, the stators have been subject to protein engineering approaches for many years, in particular the synthesis of chimeric stator constructs that enable the motor of *E. coli*, natively proton-driven, to be powered by sodium ion flow[8]. The majority of stators are proton driven, but many that are sodium-driven can be found in nature, and this divergence is presumed to have occurred in the distant past[9-11]. Past reports have argued that H^+-coupled motility diverged from Na^+-coupled machinery in ancestral times[12], but the molecular basis for this adaptation, and the evolutionary landscape that constrains stator adaptation remains unclear.

In order to simulate the effects of natural evolution on stator adaptation we designed an experiment where an *E. coli* strain, expressing only a sodium-powered stator, would be introduced to a non-lethal environment (soft agar swim plate) which lacked the power source for the stator (Na^+). Our hypothesis was that the population would undergo selection for upmotile variants, adapting its stators to function in the new environment.

We used genomic editing techniques (no-SCAR CRISPR/Cas9[13] and λ-Red[14]) to replace the native *motA motB* stator genes of the *E. coli* BFM with chimeric sodium-powered *pomA potB* (henceforth *pots*) stator genes derived from *V. alginolyticus*[8]. We transplanted the *pots* stator genes at the same location and orientation of the native *motA motB* locus to preserve the native genomic context of the motile RP437

E. coli strain. We then examined which genetic changes occurred during growth on soft-agar in depleted sodium, that is, under selective pressure for proton-driven motility. We performed our directed evolution experiments of our *pots E.coli* strain in the absence of antibiotics to avoid additional, undesired selective pressures [15].

RESULTS

Preparation and Directed Evolution of a Na^+ powered E.coli strain

The RP437 strain was edited to carry the chimeric *pomApotB* stator genes in place of the native *E. coli motAmotB* genes (Fig. 1A) via the no-SCAR Method[13] and traditional λ-Red recombineering respectively[14] (Supplementary Fig. 1&4). Following verification of successful editing by colony PCR and Sanger Sequencing (Supplementary Fig. 2AB), a no-SCAR Pots clone was selected and tested on swim plates (Fig. 1B). The edited strain was able to swim on sodium-rich (85 mM NaCl) soft agar plates but not on potassium-rich sodium-poor (67 mM KCl, ~8 mM [Na^+]) plates (Fig. 1B). This edited strain exhibited the same swimming behaviour as the control stator-less strain with motility restored via an inducible plasmid vector that could express the *Pots* construct (RP6894 Δ*motAmotB* + pSHU1234, hereby pPots).

We next challenged this *pots* strains to survive on K^+ based soft agar for prolonged periods (Fig. 1C). Motile subpopulations arose spontaneously from inoculated colonies within a few days. Cells from the edge of these motile flares were passaged onto fresh swim agar for up to 5 passages at 3-4 days intervals (Supplementary Fig. 5). When multiple flares occurred in a single swim ring, each was individually passaged (Fig. 1C), and could be recapitulated (Fig. 1D). Directed evolution consistently generated swimming flares when *pots* clones were cultured on agar containing yeast extract and tryptone (~8 mM [Na^+]), but not on minimal media (~ 1mM total [Na^+]) or when the *pots* construct was expressed via a plasmid (Supplementary Fig. 6). One *pots* strain generated using λ-Red methods[14], which carried the native *V. alginolyticus pomA* promoter, also successfully produced flares (Supplementary Fig. 4).

Lineages were selected for whole-genome sequencing (WGS) after a preliminary screening for mutations in the stator genes by Sanger-sequencing PCR amplicons spanning the genomic *pomApotB* locus (Fig. 2A). Variant calling to the MG1655 reference genome was used to compare single nucleotide polymorphisms (SNPs) between members of the same lineage. Our intended *pomApotB* edit was the only

difference between the RP437 and *Pots* genomes, indicating that neither no-SCAR nor λ-Red editing had resulted in off-target edits (Fig. 2A). 153 SNPs were called as variants between our experimental parent RP437 and the MG1655 reference which were shared across all lineage members (Supplementary Table).

Several lineages whose descendants could swim in reduced sodium had mutations at the *pots* locus (L3.3-4-5: PotB G20V; L6.4-5: PomA L183F; L8.3-4-5: PotB G20W). In contrast, lineages passaged only on 85 mM Na^+ agar (L1 & L2) accumulated mutations not in stators but in the flagellar components. Lineages passaged on ~8 mM sodium-poor agar whose descendants could not swim (L4) had no mutations on any flagellar genes.

To examine mutation reproducibility in the stators at higher throughput, we subjected 55 *pots* colonies to directed evolution in 8 mM [Na^+] agar. These yielded a total of 42 flares within the first 3 days of incubation, which were then passaged four more times at 3-day intervals. At the end of this experiment we selected the 20 terminal lineage members which produced the largest swim rings and Sanger-sequenced them at the *pots* locus (Supplementary Fig. 7). For these we observed a total of 5 mutations in *pomA* (S25C, D31N, P177A, P177Q and L183F) and one more new mutation in *potB* (L36Q).

Over the course of these experiments, we found that three stator residues underwent mutation at the same site twice (PomA L183F (2x), PomA P177A & P177Q, PotB G20V & G20W). WGS revealed that the *pitA* gene had mutated in three separate lineages (L2.5, L3.5, L8.5) with one of the mutations occurring twice (PitA W112*Stop).

To test for the capacity for reversion, we took sequenced lineages that swam in 8 mM [Na^+] agar (L3.3-4-5, L6.4-5, L8.3-4-5) and reintroduced them to an environment with 85 mM [Na^+] (Supplementary Fig. 7C). After 10 rounds of daily passaging, no reversion in the mutants that had enabled low-sodium swimming was observed, with only a single additional mutation gained: a *potB* T21A mutation in the terminal descendant of *potB* G20W *pitA* W112*stop (L8.5).

We further tested whether evolution could be more easily directed on minimal media when starting from a more favourable vantage. We examined all stator mutants that swam on 8 mM [Na^+] plates in conditions of further sodium scarcity (minimal media: 1 mM [Na^+]). Initially, only the strains with *potB* G20V and *pomA* P177Q mutations

could swim, and this capacity was maintained following five passages over 12 days. Sanger sequencing revealed that the terminal descendant of p*otB* G20V *pitA* G432R mutant (L3.5) gained a further mutation in *pomA* (M20L) (Supplementary Fig. 7B). A summary of all stator gene mutations obtained from all directed evolution experiments is provided in Fig. 2D.

Finally, we characterized rotational phenotypes of the parent and evolved strains in the presence and absence of sodium using a tethered cell assay (Fig. 2B, Supplementary Fig. 8). The rotation speeds of single cells were measured under sodium-free 67mM KCl or 85mM NaCl buffer conditions and also tested in presence of 100 μM of the sodium-blocker phenamil[16]. The *potB* G20V (L3.3) actively rotated in sodium-free buffers and in presence of 100 μM Phenamil (Fig. 2B) – indicating sodium-free rotation and a disrupted phenamil binding site (Fig. 2B). We further confirmed this phenotype was reversible in single cells by tracking rotation of individual tethered cells as the buffers were sequentially exchanged (Supplementary Fig. 9).

We confirmed the PotB G20V H^+-powered phenotype by introducing the same point mutation (GGG to GTG) on our plasmid vector (pPots) and testing motility in tethered cell assay when the protein was expressed in the stator-less Δ*motAB* RP6894 (Fig. 2C).

Finally, we mapped mutants to their homologous position on the recently published high-resolution *B. subtilis* $MotA_5B_2$ structure[17] (Fig. 2EF). All stator mutations accumulated at sites proximal to or within the predicted ion-transport pore, at the interface between the PotB transmembrane domain and the third and fourth transmembrane domains of PomA (Fig. 2F).

DISCUSSION

In our experiments we observed repeated mutation around the pore of the stator complex in response to ion-scarcity in the cell's surrounding environment. We confirmed phenotypic changes by measuring rotation in the absence and presence of the sodium channel blocker phenamil. Our strains adapted quickly to drive rotation in a sodium-poor environment within 2 weeks, indicating that the stators are highly adaptive.

Previous reports have shown that bacterial motility can adapt[18] and be rescued[19] via remodelling of the flagellar regulatory network. Ni et al. observed that evolutionary

adaptation of motility occurs via remodeling of the checkpoint regulating flagellar gene expression[18]. Their experiments tracked adaptive changes in swim plates, matching our experiments, however their only selection criteria were for improved swimming in an unhindered swimming population. In agreement with our results (*fliM* A161V), they found *fliM (*M67I and T192N*)* to be the amongst the first genes to mutate in the improved swimmer population but they did not report any changes in *flgL* (ΔA57-Q58), nor, significantly, did they see any mutations in any stator genes. Flagellum-mediated motility also appears to be naturally robust to the loss of regulatory factors, such as the enhancer-binding protein fleQ in *P. fluorescens*, which function can be substituted by distantly related homologous proteins[19].

In contrast, our *E. coli pots* strain faced selective pressure from ion scarcity. Our scenario is reminiscent of previous semi-solid agar experimental evolution studies on the adaptation of antibiotic resistance and recapitulates similar results. In the MEGA plate experiments of Baym et al., they similarly saw that the phosphate transporter *pitA* was repeatedly mutated, often to a frameshifted or nonsense variant[15]. In a similar experiment, the isocitrate dehydrogenase *icd* was also seen to mutate often[1].

Mutations in stators are known to affect ion usage and may confer dual-ion coupling capacity. For example, the substate preference of the *B. alcalophilus* MotPS stator (Na^+/K^+ and Rb^+) was changed with the single mutation M33L in MotS, causing the loss of both K^+- and Rb^+-coupling motility in E. coli[20]. Similarly a bi-functional *B. clausii* MotAB stator (Na^+/H^+) triple mutant (MotB V37L, A40S and G42S) was selective only for sodium ions while the combination of mutations G42S, Q43S and Q46A made MotB selective only for H^+ [21].

Except the previously reported variant *pomA* L183F[22], none of the other mutations we report have been observed in previous studies involving random mutagenesis in *motB* using ethylmethane sulfonate[23], or by mutagenesis in the *pomA* gene by using hydroxylamine[24], or in *potB* using error-prone PCR[25]. Adaptation of plasmid-encoded stator genes[12,26] has been previously reported. However, a distinct advantage of editing stator genes directly on the *E. coli* genome is that we can direct the evolution of sodium-stators *in vivo* and without antibiotics – something not possible in wild-type *Vibrio sp.* since the cells do not survive at low sodium. Conversely, it is difficult to direct evolution towards reversion because it is not possible, particularly in *E. coli*, to drastically reduce the proton concentration to incentivise the stators' use of sodium. Nevertheless, the fact that no revertants were

observed agrees with previous work suggesting that requirements for Na^+ binding are more strict than for H^+ binding, and that mutations that convert a sodium powered motor to a proton powered motor are more accessible than the reverse[27,28].

We observed a convergence of mutations on the stator genes and even to the very same nucleotide (GAG (L) to GAA (F) in two separate *pom*A L183F lineages). Since this was from a clonal population under identical environmental constraints, it suggests that adaptation of the stators is prioritized in changing environments. Mutation of pore-proximal residues into hydrophobic residues (eg. G20V) might hint at a mechanism for varying constrictions in the pore to alter the efficiency of ion binding.

Motility confers a fitness advantage that is worth significant energetic investment despite the high cost of synthesizing the flagellar machinery[4,29]. This advantage can only be seized if the correct ions are available for stator-conversion into torque. CRISPR/Cas9 has become a widespread method used for precise genomic edits, yet the reversion of such edits appears rapid and gene targeted. Here, ion scarcity supplied a strong selective pressure that allowed us to identify novel mutations correlated with altered ion-specificity. Our transplant of an unfit protein and the cells' rapid reversion of this edit demonstrates tight evolutionary regulation of the stator subunit in an ancient molecular complex.

MATERIALS AND METHODS

Starting strains and plasmids.

E. coli strain RP437 was used as the parent strain for genomic editing experiments[30]. The pSHU1234 (pPots) plasmid encoding *pomA* and *potB*[25] was used as the template to generate the double stranded donor DNA. This was used to replace the *motA* and *motB* gene on the RP437 chromosome. Liquid cell culturing was done using LB broth (NaCl or KCl, Yeast Extract, Bacto Tryptone). Cells were cultured on agar plates composed of LB Broth and 1% Bacto Agar (BD, U.S.A.). Swim plate cultures were performed on the same substrates adjusted for agar content (0.3% Bacto Agar).

Editing E. coli with Cas9-assisted Recombineering.

This procedure was adapted from the no-SCAR method[13] . The target strain to be edited (*E.coli* RP437) was sequentially transformed first with the pKD-sgRNA-3'MotA (Sm^+) plasmid, encoding a sgRNA sequence directed at the 3' end of *motA*, and then

with the pCas9cr4 (Cm^+) plasmid to yield a parent strain harboring both plasmids. The overlap extension PCR technique[31] was employed to assemble linear double stranded DNA molecules (dsDNA) using 3 starting dsDNA fragments. The resulting donor DNA was electroporated in the plasmid-bearing host and the successfully edited clones were selected via colony PCR and Sanger sequencing of the *motAB* locus. A list of primers and PCR protocols used in this work is provided in Supplementary Fig. 10.

Construction of Pots by λ-Red Recombineering

Chromosomal replacement from *motAmotB* to *pomApotB* was achieved by using a λ Red recombination system, with plasmid pKD46 encoding the Red system and positive selection for the recovery of swimming ability[32]. Motile clones were selected by isolating motile flares on swim plates (Supplementary Fig. 4A).

Tethered cell assay preparation and analysis

The tethered cell assay was performed as previously described[33]. The tethered cells time lapse videos were recorded at 40x magnification on a phase contrast microscope (Nikon). Time lapse videos were collected using a camera (Chameleon3 CM3, Point Grey Research) recording 20 s-long videos at 20 frames per second. Time lapse videos were collected using a camera (Chameleon3 CM3, Point Grey Research) recording 20s-long videos at 20 frames per second. Single cell tracking experiments were collected using a camera (DMK21AU618, Imaging Source) recording 10s-long videos recorded at 60 frames per second. Custom LabView software[10,25] was employed as previously reported to estimate specific rotational parameters of the tethered cells such as rotation frequency (speed), clockwise and counterclockwise bias and switching frequency. Visualization of the data was performed using Graph Pad Prism 8.

Single Nucleotide Polymorphism (SNP) analysis

Whole genome sequencing of 22 *E. coli* strains was performed using a MiSeq 2x 150bp chip on an Illumina sequencing platform. Sequencing was carried out at the Ramaciotti Centre for Genomics, Kensington and delivered as demultiplexed fastQ files (Quality Control: >80% bases higher than Q30 at 2×150 bp). The SNP calling and analysis was performed using Snippy[34,35]. The short reads from sequencing were aligned to the MG1655 reference *E. coli* genome (GenBank: U00096.2) and to a synthetic genome based on MG1655, edited to contain the Pots stator sequences from pPots (*pomA*/*potB*) at the *motAB* locus.

AUTHOR CONTRIBUTIONS

PR and MABB designed and executed experiments in strain editing, molecular biology, microbiology and rotational measurement. TS and YS executed experiments in strain editing and rotational measurement. MABB executed bioinformatics surrounding variant calling. MB supervised the design, execution and writing of the project. All authors contributed to writing and revision of the manuscript.

ACKNOWLEDGEMENTS

We would like to acknowledge Myu Yoshida and Rie Ito for technical assistance.

FUNDING

YS was supported by JSPS KAKENHI (JP18H02475 and JP20K06564), MEXT KAKENHI (JP19H05404) and Takeda Science Foundation. MABB was supported by a UNSW Scientia Research Fellowship, a CSIRO Synthetic Biology Future Science Platform 2018 Project Grant, and ARC Discovery Project DP190100497.

REFERENCES

1 Fraebel, D. T. *et al.* Environment determines evolutionary trajectory in a constrained phenotypic space. *Elife* **6**, doi:10.7554/eLife.24669 (2017).

2 Roszak, D. B. & Colwell, R. R. Survival strategies of bacteria in the natural environment. *Microbiol Rev* **51**, 365-379 (1987).

3 Gude, S. *et al.* Bacterial coexistence driven by motility and spatial competition. *Nature* **578**, 588-592, doi:10.1038/s41586-020-2033-2 (2020).

4 Ni, B., Colin, R., Link, H., Endres, R. G. & Sourjik, V. Growth-rate dependent resource investment in bacterial motile behavior quantitatively follows potential benefit of chemotaxis. *Proc Natl Acad Sci U S A* **117**, 595-601, doi:10.1073/pnas.1910849117 (2020).

5 Pallen, M. J. & Matzke, N. J. From The Origin of Species to the origin of bacterial flagella. *Nat Rev Microbiol* **4**, 784-790, doi:10.1038/nrmicro1493 (2006).

6 Deme, J. C. *et al.* Structures of the stator complex that drives rotation of the bacterial flagellum. *Nat Microbiol* **5**, 1553-1564, doi:10.1038/s41564-020-0788-8 (2020).

7 Santiveri, M. *et al.* Structure and function of stator units of the bacterial flagellar motor. 2020.2005.2015.096610, doi:10.1101/2020.05.15.096610 %J bioRxiv (2020).

8 Asai, Y., Yakushi, T., Kawagishi, I. & Homma, M. Ion-coupling determinants of Na+-driven and H+-driven flagellar motors. *J Mol Biol* **327**, 453-463, doi:10.1016/s0022-2836(03)00096-2 (2003).

9 Takekawa, N. *et al.* Structure of Vibrio FliL, a New Stomatin-like Protein That Assists the Bacterial Flagellar Motor Function. *mBio* **10**, doi:10.1128/mBio.00292-19 (2019).

10 Islam, M. I., Lin, A., Lai, Y. W., Matzke, N. J. & Baker, M. A. B. Ancestral Sequence Reconstructions of MotB Are Proton-Motile and Require MotA for Motility. *Front Microbiol* **11**, 625837, doi:10.3389/fmicb.2020.625837 (2020).

11 Lai, Y. W., Ridone, P., Peralta, G., Tanaka, M. M. & Baker, M. A. B. Evolution of the Stator Elements of Rotary Prokaryote Motors. *J Bacteriol* **202**, doi:10.1128/JB.00557-19 (2020).

12 Takekawa, N. *et al.* Sodium-driven energy conversion for flagellar rotation of the earliest divergent hyperthermophilic bacterium. *Sci Rep* **5**, 12711, doi:10.1038/srep12711 (2015).

13 Reisch, C. R. & Prather, K. L. The no-SCAR (Scarless Cas9 Assisted Recombineering) system for genome editing in Escherichia coli. *Sci Rep* **5**, 15096, doi:10.1038/srep15096 (2015).

14 Datsenko, K. A. & Wanner, B. L. One-step inactivation of chromosomal genes in Escherichia coli K-12 using PCR products. *Proc Natl Acad Sci U S A* **97**, 6640-6645, doi:10.1073/pnas.120163297 (2000).

15 Baym, M. *et al.* Spatiotemporal microbial evolution on antibiotic landscapes. *Science* **353**, 1147-1151, doi:10.1126/science.aag0822 (2016).

16 Atsumi, T., Sugiyama, S., Cragoe, E. J., Jr. & Imae, Y. Specific inhibition of the Na(+)-driven flagellar motors of alkalophilic Bacillus strains by the amiloride analog phenamil. *J Bacteriol* **172**, 1634-1639, doi:10.1128/jb.172.3.1634-1639.1990 (1990).

17 Deme, J. C. *et al.* Structures of the stator complex that drives rotation of the bacterial flagellum. *Nat Microbiol* **5**, 1553-+, doi:10.1038/s41564-020-0788-8 (2020).

18 Ni, B. *et al.* Evolutionary Remodeling of Bacterial Motility Checkpoint Control. *Cell Rep* **18**, 866-877, doi:10.1016/j.celrep.2016.12.088 (2017).

19 Taylor, T. B. *et al.* Evolution. Evolutionary resurrection of flagellar motility via rewiring of the nitrogen regulation system. *Science* **347**, 1014-1017, doi:10.1126/science.1259145 (2015).

20 Terahara, N., Sano, M. & Ito, M. A Bacillus Flagellar Motor That Can Use Both Na+ and K+ as a Coupling Ion Is Converted by a Single Mutation to Use Only Na+. *Plos One* **7**, doi:ARTN e4624810.1371/journal.pone.0046248 (2012).

21 Terahara, N., Krulwich, T. A. & Ito, M. Mutations alter the sodium versus proton use of a Bacillus clausii flagellar motor and confer dual ion use on Bacillus subtilis motors. *P Natl Acad Sci USA* **105**, 14359-14364, doi:10.1073/pnas.0802106105 (2008).

22 Sudo, Y., Terashima, H., Abe-Yoshizumi, R., Kojima, S. & Homma, M. Comparative study of the ion flux pathway in stator units of proton- and sodium-driven flagellar motors. *Biophysics (Nagoya-shi)* **5**, 45-52, doi:10.2142/biophysics.5.45 (2009).

23 Garza, A. G., Harris-Haller, L. W., Stoebner, R. A. & Manson, M. D. Motility protein interactions in the bacterial flagellar motor. *Proc Natl Acad Sci U S A* **92**, 1970-1974, doi:10.1073/pnas.92.6.1970 (1995).

24 Kojima, S., Kuroda, M., Kawagishi, I. & Homma, M. Random mutagenesis of the pomA gene encoding a putative channel component of the Na(+)-driven polar flagellar motor of Vibrio alginolyticus. *Microbiology (Reading)* **145 (Pt 7)**, 1759-1767, doi:10.1099/13500872-145-7-1759 (1999).

25 Ishida, T. *et al.* Sodium-powered stators of the bacterial flagellar motor can generate torque in the presence of phenamil with mutations near the peptidoglycan-binding region. *Mol Microbiol* **111**, 1689-1699, doi:10.1111/mmi.14246 (2019).

26 Nishino, Y., Onoue, Y., Kojima, S. & Homma, M. Functional chimeras of flagellar stator proteins between E-coli MotB and Vibrio PomB at the periplasmic region in Vibrio or E-coli. *Microbiologyopen* **4**, 323-331, doi:10.1002/mbo3.240 (2015).

27 Mulkidjanian, A. Y., Galperin, M. Y., Makarova, K. S., Wolf, Y. I. & Koonin, E. V. Evolutionary primacy of sodium bioenergetics. *Biol Direct* **3**, 13, doi:10.1186/1745-6150-3-13 (2008).

28 Hase, C. C., Fedorova, N. D., Galperin, M. Y. & Dibrov, P. A. Sodium ion cycle in bacterial pathogens: evidence from cross-genome comparisons. *Microbiol Mol Biol Rev* **65**, 353-370, table of contents, doi:10.1128/MMBR.65.3.353-370.2001 (2001).

29 Colin, R. & Sourjik, V. Emergent properties of bacterial chemotaxis pathway. *Curr Opin Microbiol* **39**, 24-33, doi:10.1016/j.mib.2017.07.004 (2017).

30 Parkinson, J. S. Complementation analysis and deletion mapping of Escherichia coli mutants defective in chemotaxis. *Journal of Bacteriology* **135**, 45-53 (1978).

31 Higuchi, R., Krummel, B. & Saiki, R. K. A general method of in vitro preparation and specific mutagenesis of DNA fragments: study of protein and DNA interactions. *Nucleic Acids Res* **16**, 7351-7367, doi:10.1093/nar/16.15.7351 (1988).

32 Kinosita, Y. *et al.* Distinct chemotactic behavior in the original Escherichia coli K-12 depending on forward-and-backward swimming, not on run-tumble movements. *Sci Rep* **10**, 15887, doi:10.1038/s41598-020-72429-1 (2020).

33 Nishiyama, M. & Kojima, S. Bacterial motility measured by a miniature chamber for high-pressure microscopy. *Int J Mol Sci* **13**, 9225-9239, doi:10.3390/ijms13079225 (2012).

356 34 Bush, S. J. *et al.* Genomic diversity affects the accuracy of bacterial single-nucleotide
357 polymorphism-calling pipelines. *Gigascience* **9**, doi:10.1093/gigascience/giaa007 (2020).
358 35 Seemann, T. Snippy: fast bacterial variant calling from NGS reads. *Internet*
359 **https://github.com/tseemann/snippy** (2015).

360

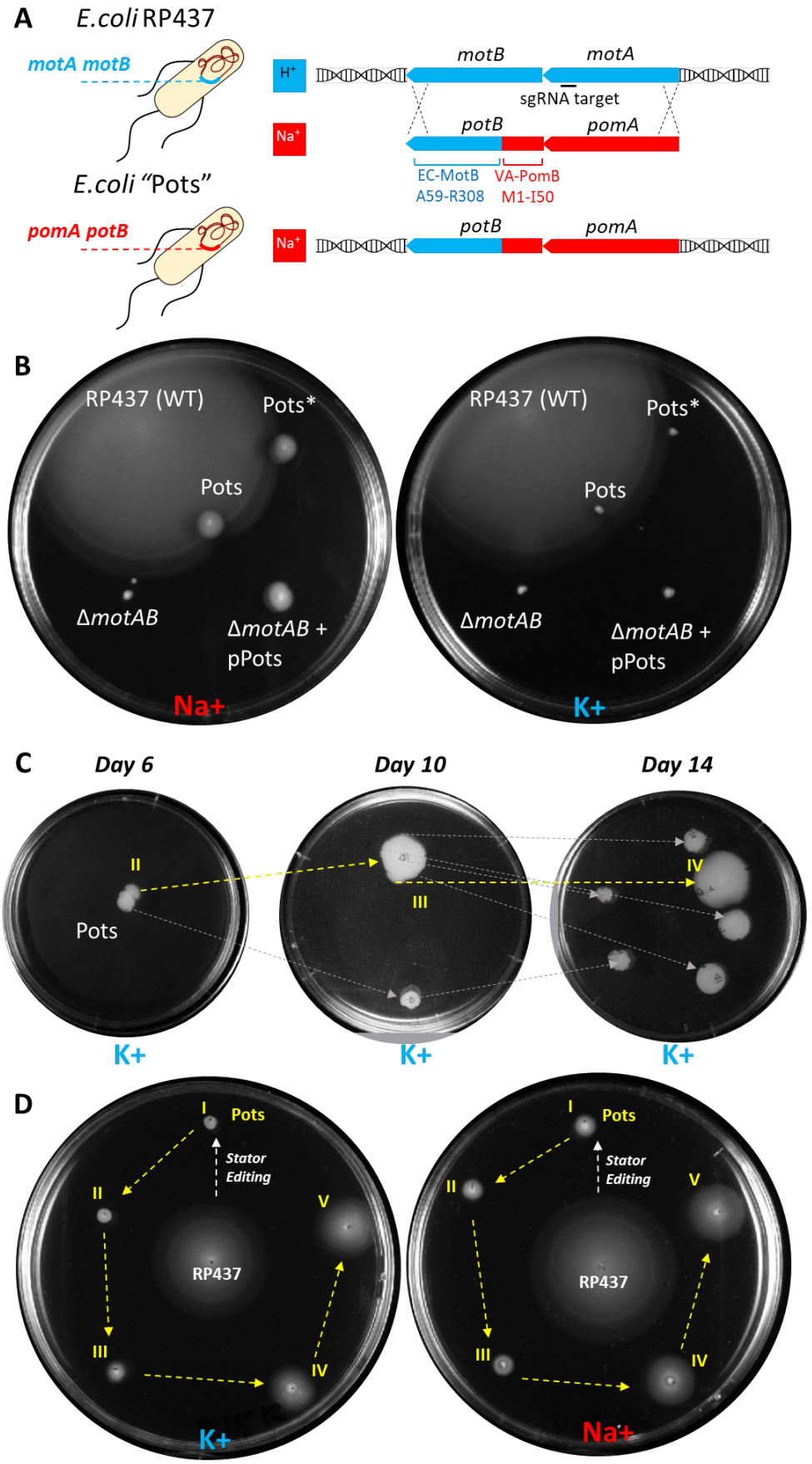

Figure 1. BFM stator editing and recapitulated directed evolution. A) Schematic of E. coli RP437, carrying a proton-powered stator set (*motA motB*), undergoing an

homologous recombination-catalysed editing process to replace *motAB* with the sodium-powered chimeric stator *pomA potB* ('pots') via a dsDNA donor. The chimeric Pots construct consists of DNA that encodes pomA from *V. alginolyticus* (VA) and a spliced B subunit encoding for *Vibrio* p omB amino acids M1-I50 fused in frame to *E. coli* (EC) motB A59 - R308 (now potB A51 – R300). B) Soft agar swim plate assay to assess bacterial motility. The strains indicated above were inoculated on 0.3% Agar prepared with either NaCl LB (left) or KCl LB (right) media and incubated at 30°C for 24 hrs. The plates contain no antibiotics and 0.4% arabinose to induce expression from pPots. Strains: RP437 (WT, parent strain), Pots* (not-fully cured, carries plasmid pCas9cr4), Pots (cured of all plasmid), Δ*motAB* (*E.coli* RP6894) with or without pPots (pSHU1234, Cm^+, encoding the pomApotB construct under arabinose induction). C) Directed evolution experiment plates. A single Pots colony was innoculated on a K^+ soft agar plate and incubated at 30˚C until flares developed. The edge of the flare was then transferred onto a fresh plate and allowed to spread radially until it was again transferred at 4-day intervals. Yellow arrows indicate an improved swimmer subpopulation being propagated. Grey arrows indicate other portions of the colony being propagated. D) Full recapitulation of the evolved lineage shown in (C). Lineage members were inoculated on soft LB agar with or without sodium from glycerol stocks and incubated for 24 hrs at 30°C. Parent strain RP437 is also included in the centre of the plate as control. The phenotypic effect of stator replacement is highlighted by the white arrows. Passages 1 to 5 of the directed evolution experiment are indicated in roman numerals and each passage highlighted by yellow arrows. These passages correspond to: I = Pots, II = L4.2, III = L5.3, IV = L6.4 and V = L6.5 in Fig. 2, respectively.

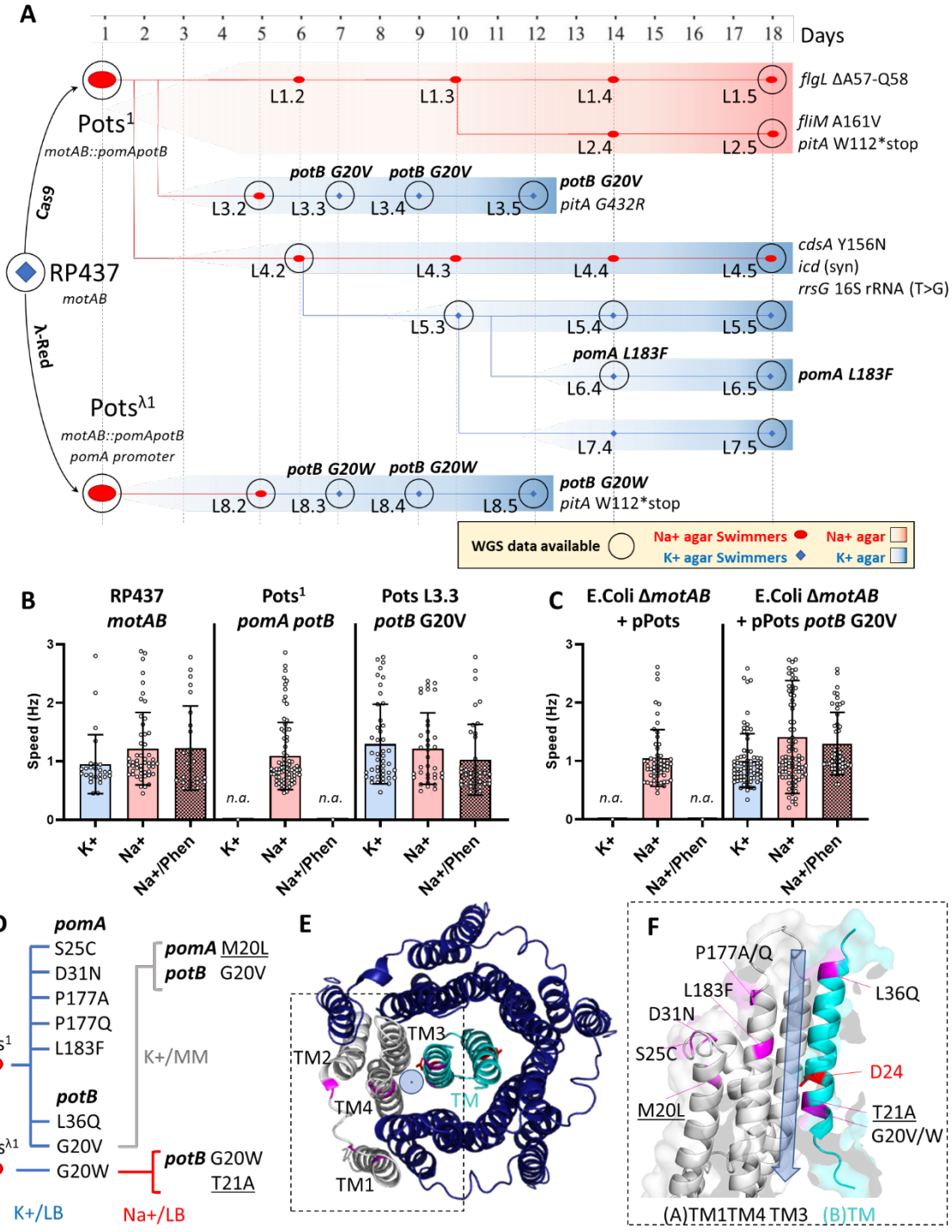

Figure 2. Sequencing and phenotyping of evolved lineages. A) Schematic of directed evolution experiments. The lineage members in the diagram are color-coded based on their ability to swim on either a Na^+ -based substrate (red ellipse) or K^+-based swim agar (blue diamond). All lineage members labelled in blue retained their ability to swim on Na^+-rich soft agar. Lineages passaged on K^+ agar are highlighted by a blue gradient bar, while lineages passaged on Na^+ agar are highlighted by a red gradient bar. All strains were locally Sanger sequenced at the *pomApotB* locus, but 21

strains, indicated by black circles, underwent whole genome sequencing (WGS). Lineage number and passage are indicated: ie L1.3 indicates the first lineage and the third passage of a motile flare from an initial inoculation site. SNPs identified via variant calling relative to reference genome of MG1655 are annotated next to each respective lineage member. Highlighted genes other than *pomA* and *potB*: *pitA* (metal phosphate:H^+ symporter), *flgL* (flagellar hook-filament junction protein 2), *fliM* (flagellar motor switch protein), *cdsA* (cardiolipin-diglyceride synthase), *icd* (isocitrate dehydrogenase), *rrsG* (16S ribosomal RNA). B) Single cell speed measurements using the tethered cell assay measured in Hz (revolutions/s). Blue bar indicates speed in 67 mM KCl motility Buffer, red bar: 85 mM NaCl motility Buffer; red patterned bar: 85 mM NaCL + 100 μM phenamil motility buffer. Number of cells analysed per condition (from left to right): RP437: 27, 51, 25; pots: n.a, 78, n.a; pots *potB* G20V 45, 36, 39 (n.a. indicates no visible rotating cell). Error bars indicate Standard Deviation (S.D.). C) Single cell speed measurements using the tethered cell assay in RP6894 Δ*motAB* strain co-expressing *pomA* and *potB* G20V from pPots plasmid. Blue bar indicates speed in 67 mM KCl motility buffer, red bar: 85 mM NaCl motility buffer; red patterned bar: 85 mM NaCl + 100 μM phenamil motility buffer. Number of cells analysed per condition (from left to right): (Δ*motAB* + pPots: n.a., 32, n.a; Δ*motAB* + pPots *potB* G20V: 40, 63, 48). Error bars indicate S.D. D) Graphical summary of stator gene mutations detected across all directed evolution experiments and the growth conditions under which these mutations arose. LB indicates agar containing Yeast extract and Tryptone. MM indicates agar in minimal media. Mutations in a subsequent generation are underlined. E) View from the extracellular side of the transmembrane portion of *B. subtilis* $MotA_5B_2$ stator complex (PDB: 6YSL). One monomer of subunit A is coloured in white and the TM domains of the B subunits are coloured in cyan. Mutant sites obtained in the directed evolution experiments are labelled in magenta, the catalytic aspartate residue essential for function is highlighted in red. The light blue circle indicates the predicted location of the ion transport pore (inward conduction). F) side view of the area highlighted by the dashed box in (E). Homologous residue location derived from protein sequence alignments. Primary mutation sites are indicated in black, while secondary mutation sites are underscored. The arrow at the interface between (A)TM3-4 and (B)TM indicates the predicted location of the ion transport pore.